International Conference on Space Optics—ICSO 2018

Chania, Greece

9–12 October 2018

Performance validation of a high-bandwidth fine steering mirror for optical communications

G. Witvoet

S. Kuiper

A. Meskers

Performance validation of a high-bandwidth Fine Steering Mirror for optical communications

G. Witvoet[*ab], S. Kuiper[a], A. Meskers[a]

[a]TNO, Dept. of Optomechatronics, Delft, The Netherlands; [b]Eindhoven University of Technology, Dept. of Mechanical Engineering, Eindhoven, The Netherlands

ABSTRACT

This paper presents the first test results of a novel Fine Steering Mirror (FSM) for optical communication terminals. The FSM utilizes efficient variable reluctance actuators, tailored for the specific application, making it highly compact and power efficient. The test results demonstrate a high dynamical performance of >1.7kHz closed-loop bandwidth, and an optical angular range of more than ±2˚ in two axes. The actual optical angular jitter is less than 1.5 µrad. These numbers demonstrate that this FSM is highly suitable for the evolving field of inter-satellite laser communications.

Keywords: Optical satellite communication, active optics, pointing, fine steering, feedback control

1. INTRODUCTION

Over the last couple of years optical communication has emerged as a novel data transfer technology, promising secure and high data-rate connections over long distances. It is therefore considered a key enabler for future high data communications between satellites, unmanned aerial vehicles (UAVs) and ground stations. Successful communication over several thousands of kilometers depends heavily on the pointing accuracy between the transmitter and the receiver; for such large distances accuracies of typically a few µrads is required. This pointing has to be maintained in the presence of various sources of misalignments, such as atmospheric aberrations and disturbances on the vehicle or satellite platform stemming from active elements, which could have a relatively high-frequency signature. In the communication terminal, these beam misalignments are measured with a tracking sensor and closed-loop compensated by a Fine Steering Mirror (FSM). A similar mirror, the Point Ahead Assembly (PAA), generates an offset angle between the transmitted and receiving beams in order to compensate for the satellite motion during the laser light running time.

The FSM has a direct influence on the pointing performance of an optical communication terminal and hence the requirements for an FSM are quite challenging. For space-based terminals an FSM needs to be accurate with very low jitter over a relatively large stroke, it should achieve a very high tracking bandwidth, and it should be commercially attractive, meaning it should be low in size, weight and power (SWaP), and have low recurring cost. There are several FSMs commercially available, based on either Lorentz actuation[1,2], piezoceramics[3], or variable reluctance[4]. When it comes to space-based terminals for high data-rates however, these solutions are either too inefficient and voluminous, do not provide sufficient stroke and/or accuracy, or are not space-qualified. To this end, the Netherlands Organisation for Applied Scientific Research (TNO) has developed a double-axis FSM[5], targeted to comply with the challenging requirements stemming from the communication terminals under development within their optical communications program[6]. This paper shows a first fully functional and representative prototype of this novel FSM and presents the first dynamic tests results, thereby validating its dynamic performance in terms of bandwidth and jitter.

The presented FSM is highly compact with an overall dimension of Ø27x30mm and a usable mirror aperture of Ø20mm, which can optically point a beam over more than ±2˚ in two axes. The custom-developed actuators are based on the magnetic reluctance principle, which allows for high efficiency in terms of force per volume and force per unit power. The mirror angle is feedback-controlled over two sets of eddy-current sensors, which measure the mirror angle with respect to the optical bench. Frequency response measurements on the FSM demonstrate very smooth dynamics, showing hardly any noticeable higher-order modes up to the Nyquist frequency of 10 kHz, and only a limited phase drop. Thanks to this, a closed-loop tracking bandwidth of >1.7 kHz has been achieved with a first loopshaping-designed controller, while the mirror jitter is estimated to be <1.5 µrad root-mean-squared optically. This paper will discuss these dynamic identification measurements, controller design, and performance validation tests in more detail.

---

[*] gert.witvoet@tno.nl; phone +31(0)88 86 66483; www.tno.nl

2. FSM DESIGN AND REALIZATION

The mirror mechanism design[5] targets to serve both the FSM and PAA application in the communication terminal with a single device. Some of the most driving requirements during the design were therefore:

- stroke: ±2° (optical)
- closed-loop tracking bandwidth: >1 kHz
- angular jitter: ~1 µrad rms (optical)

Moreover, the FSM has been designed for low SWaP and low recurring costs, to allow for future commercially viable, compact and low power terminals for large satellite constellations.

2.1 Operating principle

To obtain a compact FSM with relatively large stroke, a very efficient actuation principle is required. The FSM therefore utilizes a novel configuration of the variable reluctance principle[4], which can be significantly more efficient than Lorentz actuation. This principle, in a slightly different configuration, is illustrated in Figure 1. A permanent magnet in the middle of a ferromagnetic joke creates two flux loops (purple dashed lines), one clockwise and one anti-clockwise, partly going through a moving element. Since the flux on both ends of the element are the same, there is no net force on it as long as the element is in its neutral position. The moving element can be actuated by sending a current through a coil on either side of the joke; this creates an additional flux loop (green dashed line), which does not go through the permanent magnet (due to its low permeability). As such, the magnetic flux on one end of the moving element will increase and decrease on the other end. This yields a net force on the element towards the air gap with the largest flux.
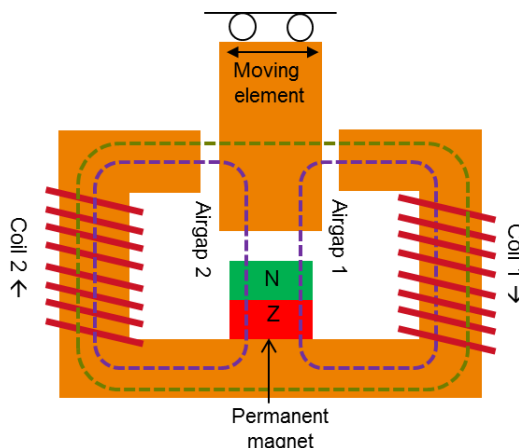

Figure 1. Illustration of the variable reluctance actuation principle. By sending a current through coil 1 and/or 2 the magnetic flux on one side of the moving element is lowered, while it increases on the other side, resulting in a net force on the element.

In the FSM design two of such jokes, in a slightly different but compact configuration, are merged perpendicularly, to allow for actuation of both tip and tilt at the same time (not stacked). The actuation is made redundant by simply utilizing separate coil windings; both coils in Figure 1 have a separate upper and lower winding, where coils 1[upper] and 2[upper] form one actuator, and coils 1[lower] and 2[lower] form the second one.

Reluctance actuation comes with a negative stiffness; if the moving element translates due to a net force, the air gap decreases, thereby further increasing the actuation force. In the FSM the mirror is therefore supported by an elastic strut, which introduces a positive mechanical rotational stiffness to overcome this issue. This strut also constraints the out-of-plane motion of the mirror; in-plane motions are constrained by an elastic membrane. The strength of the permanent magnet, the size of the air gaps and the number of coil windings have all been carefully optimized based on analytic models[5], in order to optimize between linearity, efficiency, compactness and robustness.

2.2 Realization

The actuation concept has been mechanically fitted into a tight volume, resulting in the first FSM prototype depicted in Figure 2. In this volume the metrology of the mirror has been incorporated as well, by means of two sets of eddy-current sensors, whose axes are placed under 45° compared to the actuation axes. The overall envelope is only Ø27x30mm and the total mass, including sensors, is about 61 grams. Although the prototype has not been space-qualified explicitly yet, the design has been made with space-qualification in mind, e.g. predicted launch loads and proper material and component selection has been taken into account.

To test the FSM it has been connected to a dSpace real-time control system which runs at a 20 kHz sample rate. Ordinary linear current amplifiers have been used to drive the actuators. For anti-aliasing purposes the sensor outputs are low-pass filtered by a simple analog circuit before being digitized in the dSpace system. In future space applications these components will be replaced by dedicated electronics running at even higher sample rates.
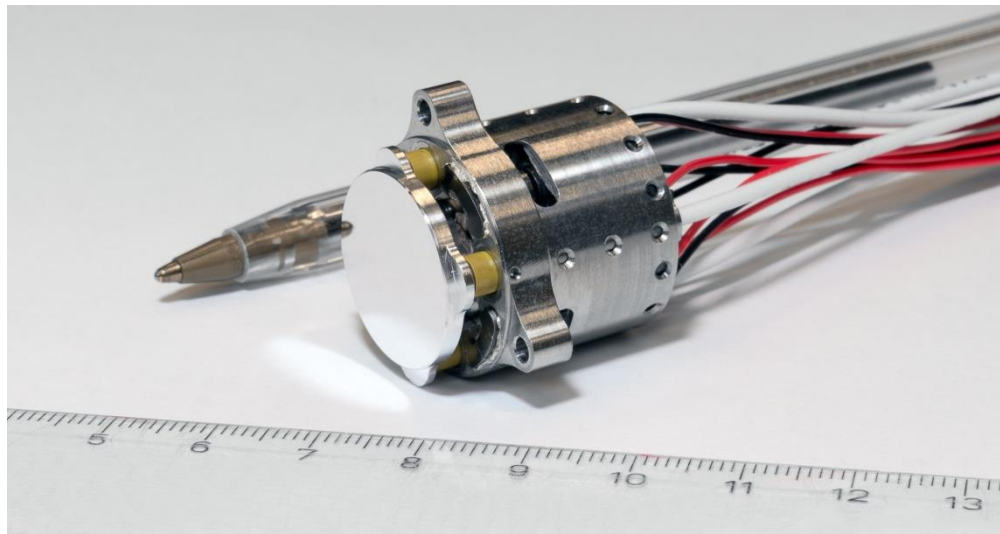

Figure 2. Picture of the actual FSM. The mirror has a usable aperture of Ø20mm, its tip/tilt is measured by the yellow eddy-current sensors incorporated in the FSM body. The black-red wires supply the coils (two redundant windings per axis). The pen and ruler illustrate the compactness of the design.
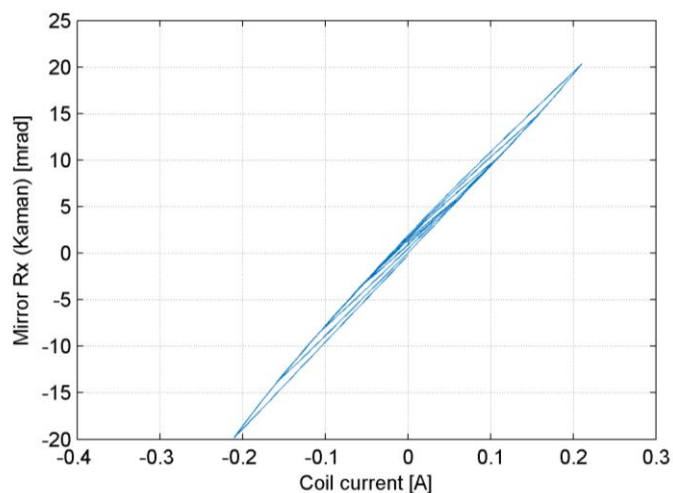

Figure 3. Result of one of the first functional tests; the FSM makes about ±20 mrad mechanical stroke (±2.3° optically) using at most ±0.21 A of current. The plot shows some about of hysteresis due to the ferromagnetic material in the FSM.

The first functional tests of the FSM involved verifying both the inputs and outputs of the mechanism. The eddy-current sensor read-outs have been calibrated using an external theodolite with sub-µrad accuracy. Furthermore, various current cycles has been sent to the coils in open loop to test the response of the mirror; the result for one of the axes is shown in Figure 3. This figure proves that the FSM has sufficient stroke (±20 mrad mechanical angle is demonstrated while ±17.5 mrad has been required), using only 0.185 A to achieve ±2° optical pointing. Each coil set has a measured resistance of 4.0 Ω, which implies that the quasi-static power consumption at full stroke is only 0.14 W. Figure 3 also shows some amount of hysteresis in open loop due to the ferromagnetic material of the jokes. However, the signature of this hysteresis is such that it can be easily compensated in closed loop (e.g. it does not include any dead-zone-like behavior).

3. DYNAMIC BEHAVIOR AND CONTROLLER DESIGN

After the stroke and power consumption have been verified, tests have been carried out to determine the possible bandwidth and accuracy of the FSM. To this end the frequency response functions (FRFs) of the FSM have been measured, a controller has been designed and closed-loop performance measurements have been carried out.

3.1 Frequency responses

The dynamic response of the FSM, by means of the FRFs, has been measured by putting small noisy signals on the coil currents and measuring the subsequent motion on the sensors. This has been repeated around numerous different nominal positions, by applying the noisy current around different offset currents. The FRFs P then follow from standard non-parametric identification techniques[7], by dividing the cross- and auto-power spectral densities of these signals. The results for the tip axis R_x are shown in Figure 4. The different colors denote the different offset positions, which thus illustrate the change in dynamics over the FSM stroke. The two fundamental eigenmodes (mirror tip and tilt) are located around 100 Hz, which vary slightly as a function of stroke due to the non-linear negative stiffness of the magnetic actuator. There seems to be another mode around 4 kHz, but this is only marginally noticeable on the response. The next significant mode (presumably a deformation mode of the mirror) seems to be located slightly above 10 kHz, but this also corresponds to the Nyquist frequency. Most importantly, between 150 Hz and 2 kHz, i.e. around the targeted bandwidth, the spread in the FRFs is negligible, thus giving constant dynamics, which is advantageous for controller design.

Note that the FSM is actually a multiple-input-multiple-output (MIMO) system, so the full FRF is a 2×2 frequency dependent matrix, also including interactions between tip and tilt. For ease of readability Figure 4 only shows one of these elements (only tip R_x). However, the interactions have explicitly been considered during the controller design.
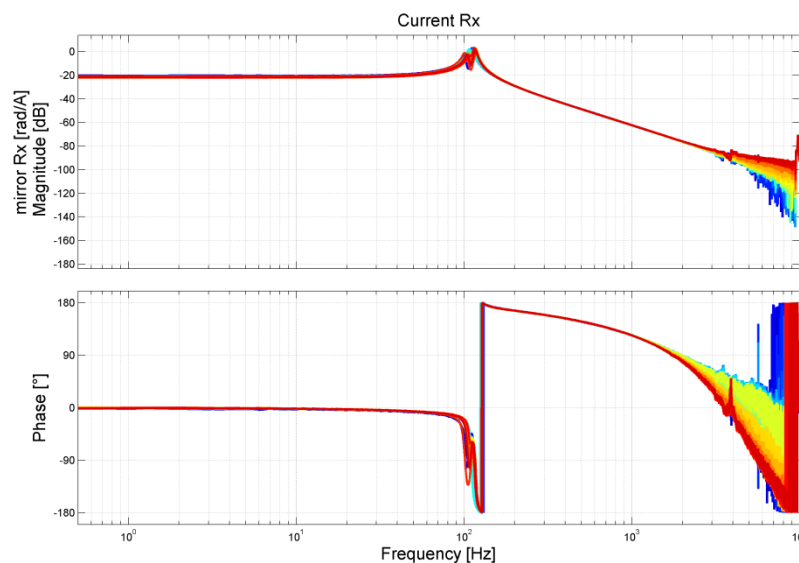

Figure 4. Measured FRFs from the tip actuator to actual mirror tip R_x around 25 different positions, covering about 60% of the FSM stroke. The FRFs for tilt R_y are not shown but are very similar to tip.

When we look to the phase of the FRFs, there is about 55° drop at 1 kHz. Close examination of the phase revealed that about 27° of this drop can be attributed to the time delay (about 1.5 samples at 20 kHz) in the total dSpace feedback system. The other half is most likely introduced by a roll-off in the magnetic circuit, which is to some extent compensable in the feedback controller.

3.2 Controller design

The identified FRFs have been used to design a controller using loopshaping techniques. Since the interaction has been assessed to be sufficiently small, decentralized control[8] is applied, where the controller is diagonal, so that there is a single SISO controller for each axis. For simplicity, the controllers for tip and tilt are chosen to be identical, thus leading to the MIMO controller $C_{\text{MIMO}} = \begin{bmatrix} C_{\text{SISO}} & 0 \\ 0 & C_{\text{SISO}} \end{bmatrix}$. Although the differences between the tip and tilt FRFs are quite small, this introduces a little bit of conservatism.

The controller C_{SISO} has been loopshaped such that it maximizes the open-loop cross-over frequencies, while maintaining a 6 dB robustness margin on both the error rejection performance (sensitivity S) and tracking performance (complementary sensitivity T). Moreover, the controller structure is kept simple; C_{SISO} is essentially a low-passed PID with an additional lead filter to compensate for the magnetic roll-off.

The controller design is visualized in Figure 5, showing the MIMO open loops PC_{MIMO} both in a Bode and Nyquist plot. These plots demonstrate closed-loop stability with sufficient margins, while achieving >600 Hz open-loop cross-over frequencies. Note that the interaction between tip and tilt is indeed small around these frequencies, which justifies the decentralized approach.
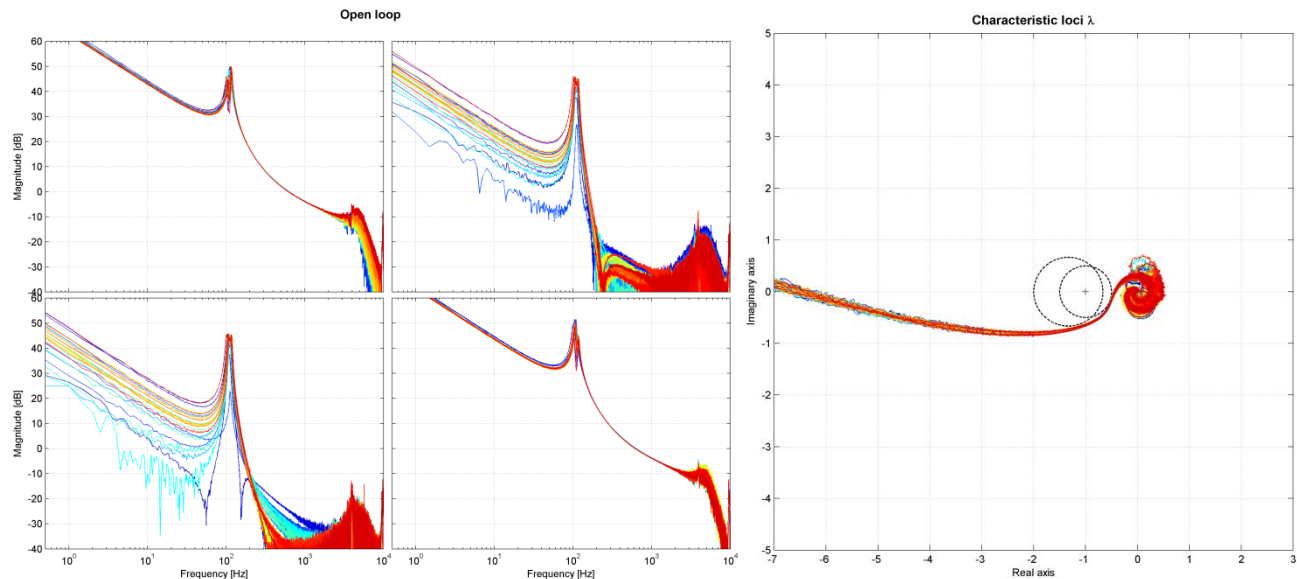

Figure 5. Illustration of the FSM controller design, in terms of the open loop PC_{MIMO}. The Bode diagram of the MIMO open loop is shown on the left, showing cross-over frequencies >600 Hz on the diagonals, and very small off-diagonals at these frequencies. The characteristic loci[8] (MIMO equivalent of the Nyquist curve) on the right prove closed-loop stability since all loci are on the right side of the point (-1,0); the two dashed circles indicate robustness margins.

4. PERFORMANCE VALIDATION

The actual performance of the FSM in terms of angular jitter depends on both the feedback performance and the external disturbances. This is illustrated in Figure 6: the true output y is affected by disturbanced d and measurement noise η and the corresponding closed-loop transfer functions. These d and η are however not exactly known, therefore first the open-loop spectrum (in stand-still) on the eddy-current sensors has been determined, shown on the left of Figure 7.
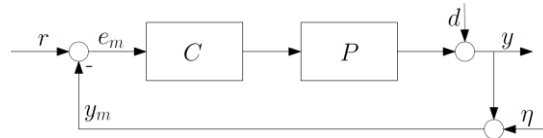
Figure 6. Generic feedback scheme, showing different propagations of disturbances d and noise η on the true output y.
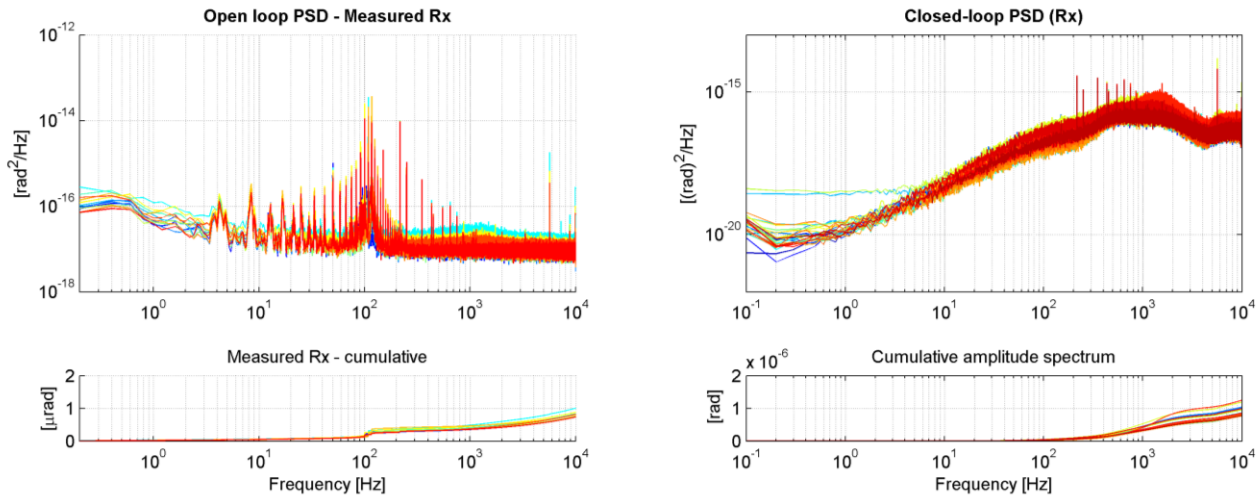

Figure 7. Open-loop (left) and closed-loop (right) performance on tip R_x as measured by the FSM eddy-current sensors. Different colors again represent different nominal positions along the FSM stroke.

This spectrum shows a certain noise floor, a slight excitation of the tip and tilt modes around 100 Hz, and various narrow spikes. The latter are probably induced by the current amplifiers, but hardly contribute to the total root-mean-squared (rms) error of about 1 µrad (mechanically). Together with the 100 Hz modes they constitute d, and are thus assumed to be compensable in feedback. The noise floor can probably be allocated to the sensors and the quantization of the dSpace system, and thus contribute to η. Again, only the results for tip R_x are shown, but the R_y results are very similar.

When the feedback loop is closed using the controller C_{MIMO} discussed in the previous section, the eddy-current sensors return the error spectrum shown on the right of Figure 7. This indeed confirms that the controller successfully rejects the excitation of the tip and tilt modes and nearly all of the spikes. As can be expected, this closed-loop spectrum takes the shape of the sensitivity function. The rms amplitude in this spectrum of about 1 µrad does not have much worth though, since it only reflects the power in the measured output y_m instead of in the real output y.

To assess the real mirror motion one would therefore need an external validation sensor to verify the output of the eddy-current sensors. Unfortunately, there was no sufficiently accurate and fast sensor available for this purpose during the FSM test campaign, hence the true angular jitter has been estimated in a different way. To this end we make a worst case assumption that all content in the open-loop spectrum on the left of Figure 7 stems from the noise η from the sensors. Since the propagation of η to the actual output y is given by the complementary sensitivity

$$T = (1 + PC_{\mathrm{MIMO}})^{-1}PC_{\mathrm{MIMO}}, \tag{1}$$

we then assume that the true mirror jitter can be estimated by filtering the open-loop spectrum with this T. Note that this is a conservative approach, since this neglects the fact that the contributions of the disturbances d in the open-loop spectrum are actually well compensated by the feedback loop. As such this approach will return an upperbound for the actual performance.

The measured complementary sensitivities T for each location that was taken an spectrum of is shown on the left of Figure 8. By using these T as a filter for the open-loop responses, the predicted true angular mirror jitters shown on the right has been obtained.
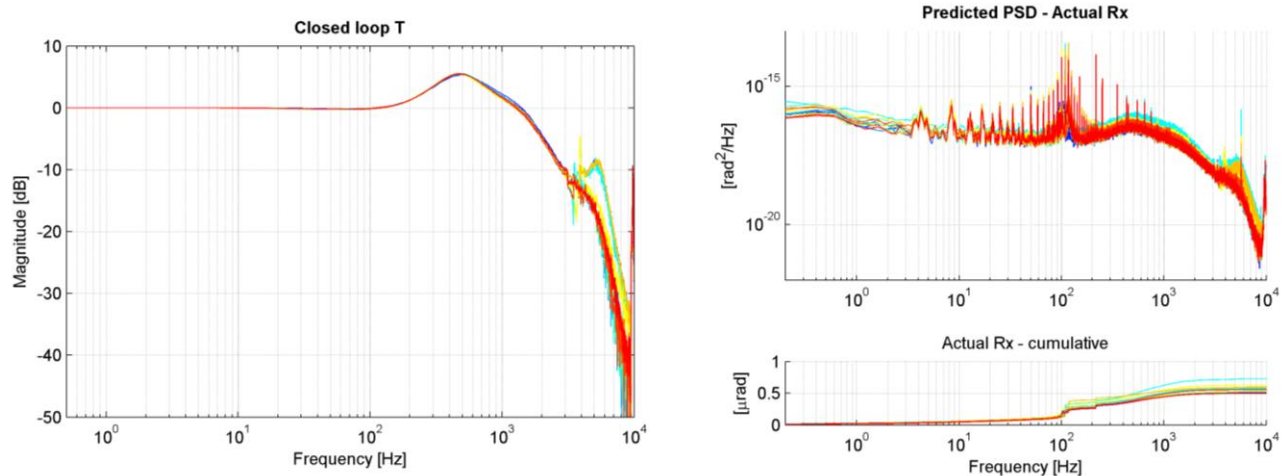
Figure 8. Measured complementary sensitivities T for tip R_x at various different position along the full FSM stroke (left) and the predicted worst case true mirror jitter using this T as a filter on the open-loop jitter (right). All spectra cumulate to less than 0.73 µrad rms of angular jitter.

It can be seen that all predicted spectra for tip R_x cumulate to less than 0.73 µrad rms (mechanically); for tilt R_y it is even less than 0.68 µrad rms (not shown). Note that a significant part of this power is caused by the tip and tilt modes around 100 Hz, which are in reality feedback suppressed, and hence do not contribute to the actual mirror jitter. The reported 0.73 µrad is thus indeed an upperbound; the true FSM jitter is even lower. We thus conclude that the optical pointing jitter of the FSM is <1.5 µrad rms, which is very close to the targeted 1 µrad.

The left plot of Figure 8 also shows the true tracking bandwidth of the FSM, determined by the -3 dB point of these plots. This bandwidth turns out to be >1.7 kHz for all positions along the FSM stroke, which complies with the >1 kHz requirement. Note that this achieved 1.7 kHz bandwidth is (partly) limited by the delay in the 20 kHz dSpace system. Future space terminals will make use of dedicated electronics in which this delay (and sample rate) can easily be further optimized, thereby enabling even higher bandwidths.

5. CONCLUSIONS

In this paper we have presented the first prototype of a novel FSM, meant to be used in future optical communication terminals. The designed FSM is smaller and lighter than what is currently commercially available, fitting in an Ø27x30mm envelope and weighing only 61 grams, thanks to the utilization of a novel configuration of efficient variable reluctance actuators. We have shown the first test results, demonstrating its 70 mrad beam deflection stroke (±2° optically), and validating its dynamic performance. With a first loopshaped controller already a closed-loop bandwidth of >1.7 kHz has been achieved, yielding <1.5 µrad rms optical pointing jitter. There is still plenty of room for further optimization of the controller and the electronics, possibly yielding even better performance. Future tests will aim to further qualify the FSM to full flight status.

ACKNOWLEDGEMENTS

REFERENCES

[1] W. Coppoolse, M. Kreinenbuehl, J. Moerschell, A. Dommann, and D. Bertsch. "Dual-axis single-mirror mechanism for beam steering and stabilisation in optical inter satellite links." In *10th European Space Mechanisms and Tribology Symposium*, (2003).

[2] H. Langenbach, and M. Schmid. "Fast steering mirror for laser communication." In *11th European Space Mechanisms and Tribology Symposium*, (2005).

[3] Physik Instrumente, "Active Optics / Fast Tip-Tilt Piezo Steering Mirrors", 2 September 2010, <http://www.pi-usa.us/products/Active_Optics_Steering_Mirrors/>

[4] D.J. Kluk, M.T. Boulet, and D.L. Trumper. "A high-bandwidth, high-precision, two-axis steering mirror with moving iron actuator." *Mechatronics*, 22(3), 257-270 (2012).

[5] S. Kuiper, W. Crowcombe, *et al*. "High-bandwidth and compact fine steering mirror development for laser communications." In *17th European Space Mechanisms and Tribology Symposium*, (2017).

[6] R. Saathof, R. den Breeje, *et al.* "Optical feeder link program and first adaptive optics test results." In *Proc. SPIE* 10524, 105240C (2018).

[7] R. Pintelon and J. Schoukens, [System Identification: A Frequency Domain Approach], Wiley-IEEE Press, Piscataway, NJ, (2001).

[8] S. Skogestad and I. Postlethwaite, [Multivariable Feedback Control: analysis and design], John Wiley, Chichester, UK, (2005).